Physics of the Solid State, 2025, Vol. 67, No. 2

16

The Role of Silver Ion Doping in the Transformation of the Phase Transition Mechanism in Vanadium Dioxide Films

© A.V. Ilinskiy[1], Ya.O. Veniaminova[2], R.A. Castro[2], V.A. Klimov[1], A.A. Kononov[2], E.B. Shadrin[1]

[1] Ioffe Institute,
St. Petersburg, Russia
[2] Herzen State Pedagogical University of Russia,
St. Petersburg, Russia
E-mail: shadr.solid@mail.ioffe.ru

Received December 25, 2024
Revised December 30, 2024
Accepted December 31, 2024

It is shown that both in doped and undoped VO_2 films the frequency position and the shape of the maxima of the frequency dependence function of the imaginary part of the complex permittivity $\varepsilon''(f)$ are determined by the values of the physical parameters of the free electron array, for which the frequency of the resonance response to the action of the probing field is due to the difference in their Maxwell relaxation times ($\tau_{\mathrm{M}} = \varepsilon\varepsilon_0/\sigma$). The same applies to the frequency position of the steps of the frequency dependence function of the real part of the permittivity $\varepsilon'(f)$ and to the position of the semicircle in the Cole-Cole diagrams. It has been established that the characteristics of the dielectric spectra indicate both a decrease in the electron concentration in the conduction band of the VO_2 semiconductor phase, caused by doping this phase with silver impurity, and an increase in the equilibrium temperature of the monoclinic and tetragonal phases. Along with this, these characteristics indicate the appearance of two types of crystalline grains with different physical properties upon strong doping with silver. It has been established that selective modification of the dielectric spectra of films by silver impurity is determined by the difference in the degree of silver ion penetration into different-sized nanocrystallites of the VO_2 film, which occurs during their synthesis. It has been shown that the cause of this phenomenon is due to the dependence of the resulting concentration of the dopant on the Laplace pressure of the nanocrystallite surface, determined by the curvature of its surface. Key words: dielectric spectroscopy, vanadium dioxide, semiconductor-metal phase transition, VO_2 films, silver doping.

Keywords: dielectric spectroscopy, vanadium dioxide, semiconductor-metal phase transition, VO_2 films, silver doping.

DOI: 10.61011/PSS.2025.02.60692.351

1. Introduction

Vanadium dioxide (VO_2) is an interesting and promising material for obtaining new scientific information, both in applied and fundamental terms. This is attributable to the fact that this material undergoes a semiconductor-metal phase transition at temperatures close to room temperature ($T_c = 67\,^{\circ}\mathrm{C}$) [1–4].

VO_2 can be synthesized on a variety of substrates in the form of thin films, both free from doping and doped with a wide range of various impurities. Such films turn out to be useful for manufacturing of a number of practical devices: thermal sensors, controlled optical transparencies, information recording devices (including optical), etc.

From a scientific point of view, the material is interesting because the semiconductor-metal PT has a complex nature in it: the Peierls structural transition takes place here along with the electronic Mott transition [5]. It should be especially noted that fundamentally new scientific results have been recently acquired using dielectric spectroscopy [6–10]. These methods, along with their practical applications, are actively used to obtain scientific information about the physical parameters of film materials. This became possible due to the development and creation of first-class dielectric spectrometers with record high sensitivity. In particular, these methods were used to study the effect of doping with a wide range of impurities on the properties of VO_2 thin films. It has been found that doping of films with elements such as W increases the PT temperature, and doping with an impurity In lowers this temperature [10]. These results are important for practical devices based on crystalline films of VO_2.

This work continues the cycle of this kind of studies. Namely, it presents the results of measuring the parameters of the dielectric spectra (DS) of thin vanadium dioxide films doped with a transition metal such as silver. The measurement results and their discussion are presented in comparison with the measurement results of specially undoped films of VO_2. It should be noted that dielectric spectroscopy selectively reveals differences in the physical parameters of the semiconductor-metal PT in the nanocrystalline grains of films of VO_2 that dramatically differ in size and are randomly mixed on the substrate surface. No other research method is capable of solving the problem of such selective sensing.

2. Experiment procedure

The DS measurement was performed using a dielectric spectrometer „Alpha-Beta Impedance Analyzer“ from Novocontrol Technologies. The sample was placed in a cell of a dielectric spectrometer between flat metal electrodes, to which a reference sinusoidal voltage $U(t)$ with an amplitude of 1 V was applied. The amplitude I_0 of the current $'I(t)$ and the phase difference φ of the oscillations $U(t)$ and $'I(t)$ were measured. These data were converted to DS using the spectrometer converter. These include:

– $\varepsilon^*(f) = \varepsilon' + i\varepsilon''$ — complex dielectric permittivity reflecting the reaction of a set of grains of a crystalline film to the action of an external periodic electric field,

– $\varepsilon''(f)$ — frequency dependence of the imaginary part $\varepsilon^*(f)$,

– $\varepsilon'(f)$ — frequency dependence of the real part $\varepsilon^*(f)$,

– $\mathrm{tg}\,\delta(f) = \varepsilon''/\varepsilon'$

– $\mathrm{tg}\,\delta(f) = \varepsilon''/\varepsilon'$ — tangent of the dielectric loss angle,

– $Z'(f)$ and $Z''(f)$ ($Z^* = Z' + iZ''$ represent the complex impedance of the sample).

The frequency dependences $\varepsilon'(f)$, $\varepsilon''(f)$ were measured in the range from 10^{-1} Hz to 10^7 Hz, the sample temperature T changed during the DS measurements from 30 °C to 100 °C in increments of 5 °C.

The studied samples are thin (80 nm) crystalline films of VO_2 synthesized using laser ablation technology on insulating mica substrates with a thickness of $40\,\mu$. A special feature of the method is the drip mode of metal deposition on the substrate. A pair of synchronous laser pulses excites flares of metal particles ejected from two identical vanadium targets in this method (purity 99.9 %). Drops of liquid metal are deposited on a mica substrate heated to 450−600 °C. Droplets are oxidized in a low-pressure oxygen stream ($4 \cdot 10^{-2}$ mm · Hg) blown along the surface of the substrate. When a dopant is introduced into VO_2, one of the vanadium targets is replaced by a target from a doping metal: in our case, silver (Ag 99.9 %). The degree of doping is judged by the relative evaporation time of each target.

3. Experimental results

DS were studied for vanadium dioxide films doped with silver in medium (3 %) and high (6 %) concentrations. However, let us consider the DS of undoped films of VO_2 for comparison at the initial stage of the analysis.

Figure 1 shows the DS of undoped films in the temperature range of 50−70 °C. The frequency dependence of the imaginary part of the dielectric permittivity $\varepsilon''(f)$ has a clearly pronounced resonant maximum at the frequency $10^{4.5}$ Hz at $T = 50$ °C (*a*), and a step in the frequency dependence of the real part of the dielectric permittivity $\varepsilon'(f)$ is clearly visible at the same frequency (*c*), while the Cole-Cole diagram $\varepsilon''(\varepsilon')$ constitutes a regular semicircle (*d*). The DS features shift towards high frequencies as the temperature increases. At the same time, the height of the peak $\varepsilon''(f)$ decreases, its half-width increases, the frequency interval occupied by the step on the graph $\varepsilon'(f)$ becomes wider, and the semicircle $\varepsilon''(\varepsilon')$ has an irregular shape. However, all the DS features return to their original shape at $T = 70$ °C, but they are located at significantly higher frequencies (a shift of more than two orders of magnitude). The cells of the spectrometer with the DS sample return to their initial state after cooling, but with some delay in temperature (the temperature hysteresis occurs). The frequency dependences of the imaginary part of the dielectric permittivity $\varepsilon''(f)$ both when the sample is heated and when it is cooled are shown for comparison in Figures 1, *a* and 1, *b*. The figure shows that the curves are very similar and mostly differ only in the temperatures of the location of the features of DS.

The analysis of the graphs shown in Figure 1 makes it possible to construct temperature hysteresis loops of the frequency position of the peak $\varepsilon''(f)$ (Figure 2, *a*).

Figure 3 shows the DS of weakly silver-doped films VO_2: Ag in the temperature range of 60−80 °C. The frequency dependence of the imaginary part of the dielectric permittivity $\varepsilon''(f)$ has a resonant maximum at the frequency $10^{4.8}$ Hz at $T = 60$ °C (*a*), and there is a pronounced step in the dependence of the real part of the dielectric permittivity $\varepsilon'(f)$ at the same frequency (*b*), while the Cole-Cole diagram $\varepsilon''(\varepsilon')$ has a shape of a distorted semicircle (*c*). The DS features shift towards high frequencies as the temperature increases, first slowly (65 °C), and then abruptly (70, 75, 80 °C). The DS features are wider compared to Figure 1, and the semicircle of the Cole-Cole diagram is more distorted. When the sample is cooled, the spectral features occupy the same frequency position, but at a lower temperature (which makes it possible to construct a temperature hysteresis loop — Figure 2, *b*).

The DS of strongly silver-doped films of VO_2: Ag shown in Figure 4 have a more complex structure in the temperature range of 60−80 °C compared with the DS shown in Figures 1, 3. Namely, a narrow maximum $\varepsilon''(f)$ appears in the low-frequency region of $f \approx 10^2 - 10^{3.5}$ Hz, the frequency position and height of which do not depend on temperature. A clear step and a large semicircle on the Cole-Cole diagram correspond to this maximum. The frequency features $\varepsilon''(f)$ and $\varepsilon'(f)$ are preserved in the high-frequency region of $f \approx 10^4 - 10^7$ Hz, although in a slightly modified form, and the second semicircle of the Cole-Cole diagram is clearly visible at high temperatures. These DS features shift towards high frequencies with increasing sample temperature, and their frequency position demonstrates the presence of temperature hysteresis — Figure 2, *c*.

4. Calculation results

The features of the dielectric spectra (DS) in this particular case are described by Debye's formulas [11]. In our case, a thin film of vanadium dioxide is synthesized

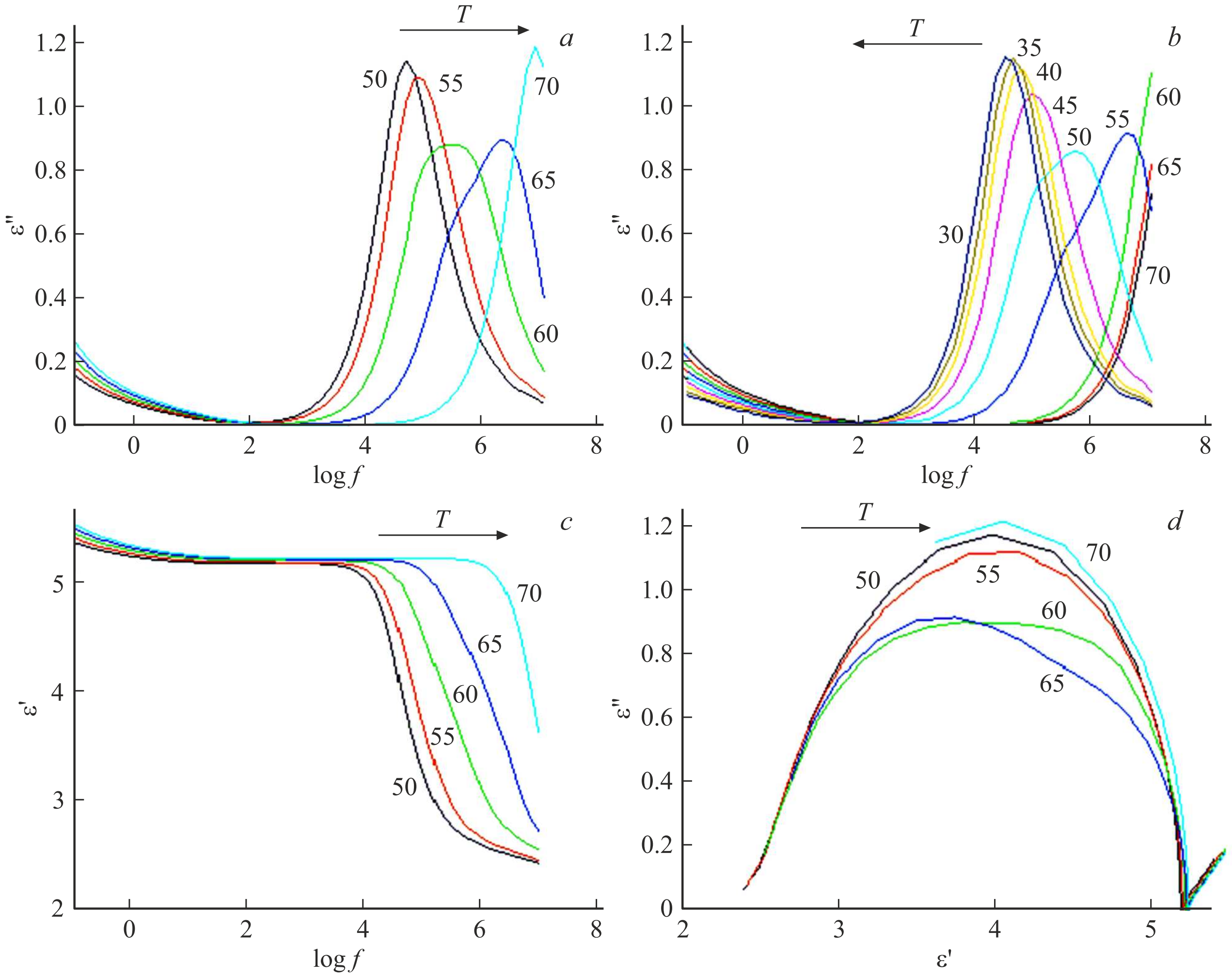

Figure 1. Frequency dependences of the imaginary part $\varepsilon''(f)$ of the complex dielectric permittivity of an unalloyed thin film of vanadium dioxide synthesized on an insulating mica substrate during heating and cooling of the film, — *a* and *b*, respectively, of the real part $\varepsilon'(f)$ — *c*, and Cole-Cole diagrams — *d* in the temperature range of 50–70 °C.

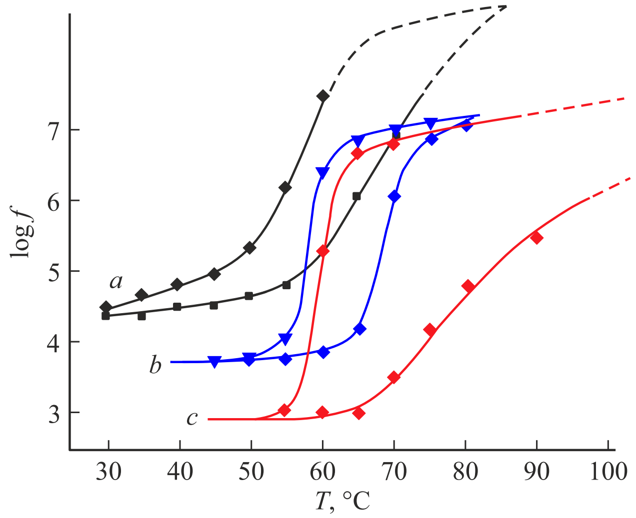

Figure 2. Temperature hysteresis loops of the frequency position $\varepsilon''(f)$, constructed according to Figure 1 — (*a*), according to Figure 3 — (*b*) and according to Figure 4 — (*with*).

on an insulating mica substrate, which eliminates the flow of through current through the sample. Therefore, Debye's formula for describing the DS in Figure 1 has the simple form:

$$\varepsilon^*(\omega) = \varepsilon_\infty + \frac{\Delta\varepsilon}{[1 + i\omega\tau_D]}, \tag{1}$$

where ε_∞ is the limit $\varepsilon'(\omega)$ at $\omega \to \infty$, $\Delta\varepsilon = \varepsilon_0 - \varepsilon_\infty$ ε_0 is the limit $\varepsilon^{'}(\omega)$ at $\omega \to 0$, i is the imaginary unit, $\omega = 2\pi f$. This formula assumes the presence in the studied material of one type of relaxers with a single relaxation time.

Figure 5 shows graphs constructed according to the formula (1) for the imaginary ($\varepsilon'' = \Delta\varepsilon \cdot \omega\tau D/[1 + (\omega\tau_D)^2]$) and real ($\varepsilon' = \varepsilon_\infty + \Delta\varepsilon/[1 + (\omega\tau_D)^2]$) parts of the complex permittivity $\varepsilon^*(\omega)$. The Cole-Cole diagram $\varepsilon''(\varepsilon')$ is also shown. The parameters of Debye's formula are empirical: all constants of frequency dependences are extracted from experimental dependences. Debye's formula describes DS well (see Figure 1) at low and high temperatures, but it does not describe the broadening of spectral features in the

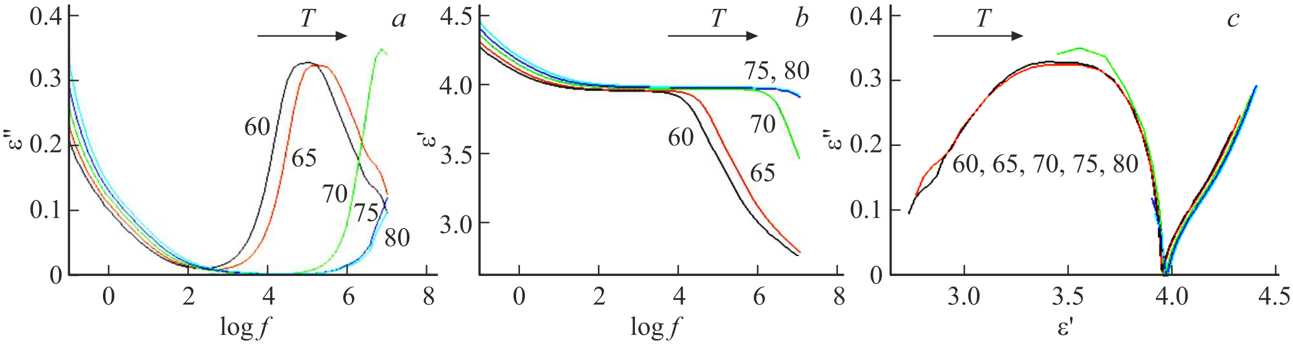

Figure 3. Frequency dependences of the imaginary part $\varepsilon''(f)$ of the complex dielectric permittivity of a weakly doped thin film of vanadium dioxide synthesized on an insulating mica substrate, — *a*, the real part $\varepsilon'(f)$ — *b*, and Cole-Cole diagrams — *c* when the film is heated in the temperature range of 60–800 °C.

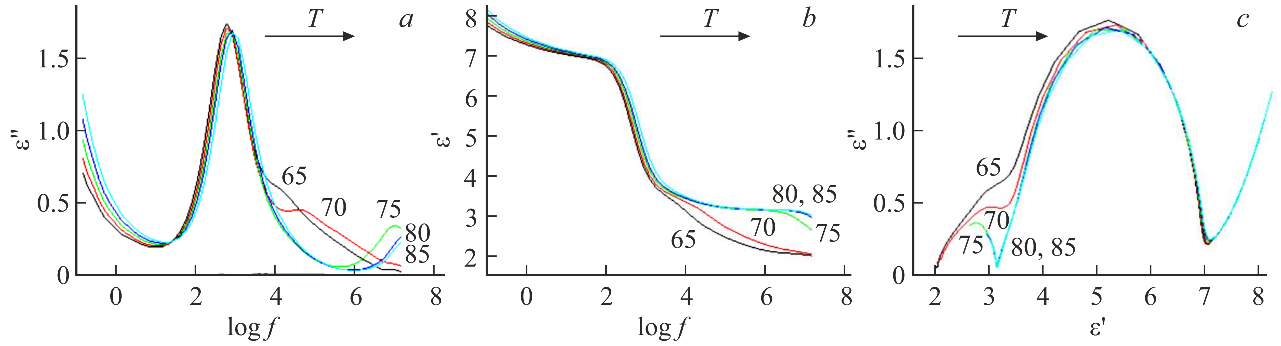

Figure 4. Frequency dependences of the imaginary part $\varepsilon''(f)$ of the complex dielectric permittivity of a highly doped thin film of vanadium dioxide synthesized on an insulating mica substrate, — *a*, the real part $\varepsilon'(f)$ — *b*, and Cole-Cole diagrams — *c* when the film is heated in the temperature range of 65–85 °C.

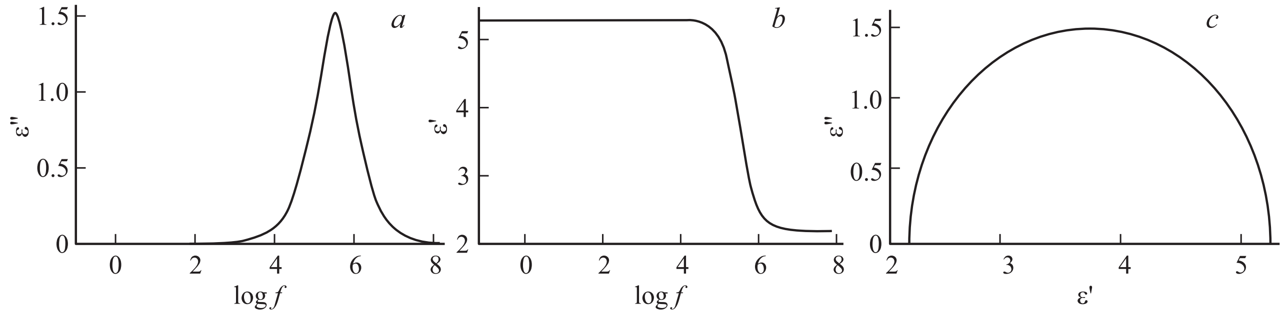

Figure 5. DS, constructed according to the formula (1).

temperature range of 60–65 °C shown in Figure 1 and does not describe the wide frequency features of DC shown in Figure 3.

We complicated the Debye's formula for describing this broadening by introducing the function $G(\tau)$ of the distribution of relaxers over relaxation times [12]:

$$\varepsilon^*(\omega) = \varepsilon_\infty + \Delta\varepsilon \int_0^\infty \frac{G(\tau)}{1 + i\omega\tau}\, d\tau. \tag{2}$$

The function $G(\tau)$ is a time dependence of the differential distribution function of the „temporary" density of relaxers $dN/d\tau$, that is, the number of relaxers per unit time interval. The integral of such a function with an infinite upper limit is equal to the total number of relaxers. A good agreement between the calculation results and the measurement results can be achieved by appropriately selecting the parameters of the function $G(\tau)$ [13]. It is reasonable to use the Gavrilyak–Negami function as a „correction" function [12] as this function contains three variable parameters: τ_{HN}, τ_{HN} and τ_{HN}. After achieving a good agreement of the calculation results with the measurement data during the fitting process, it is possible to judge the width, asymmetry and position of the maximum of the function $G(\tau)$ by the

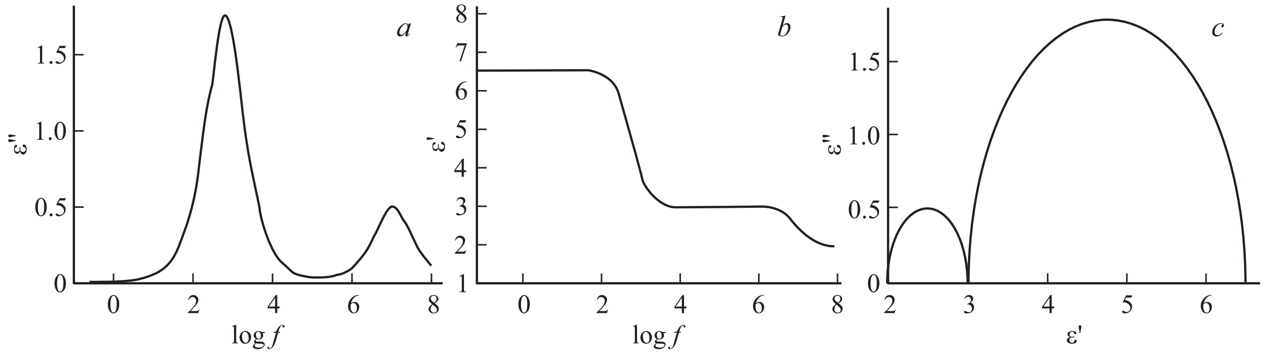

Figure 6. DS, constructed according to the formula (3). $\varepsilon_\infty = 2$, $\Delta\varepsilon_1 = 3.5$, $\Delta\varepsilon_2 = 1$, $f_1 = 102.8\,\text{Hz}$, $\tau_1 = 2.5 \cdot 10^{-4}\,\text{s}$, $f_2 = 10^7\,\text{Hz}$, $\tau_1 = 1.6 \cdot 10^{-8}\,\text{s}$.

values of these parameters. Matching the calculation results according to formula (2) [13] with the measurement results gives the following parameters of the Gavrilyak–Negami function: $\tau_{\text{HN}} = 5.10^{-7}\,\text{s}$, $\alpha_{\text{HN}} = 0.95$, $\beta_{\text{HN}} = 0.85$ for Figure 1, *a* and $T = 60\,^\circ\text{C}$; $\tau_{\text{HN}} = 1.6 \cdot 10^{-6}\,\text{s}$, $\alpha_{\text{HN}} = 0.85$, $\beta_{\text{HN}} = 0.9$ for Figure 3, *a* and $T = 65\,^\circ\text{C}$.

If DS have resonant features at two different frequencies f_1 and f_2 — Figure 4, then the Debye formula is used to describe them in the form containing two terms:

$$\varepsilon^*(\omega) = \varepsilon_\infty + \frac{\Delta\varepsilon_1}{1 + (i\omega\tau_1)} + \frac{\Delta\varepsilon_2}{1 + (i\omega\tau_2)}. \tag{3}$$

Figure 6 shows graphs constructed using the formula (3) for the imaginary $\varepsilon''(f)$ and real $\varepsilon'(f)$ parts of the complex permittivity $\varepsilon^*(\omega)$, the Cole-Cole diagram $\varepsilon''(\varepsilon')$ is also shown. The parameters of formula (3) are matched to the experimental results of Figure 4 at $T = 75\,^\circ\text{C}$.

5. Results and discussion

The occurrence of the DS features of vanadium dioxide thin films in the proposed model of their formation mechanism is associated with the frequency dependence of the parameters of the electrical response of the nanocrystalline system to the action of an external sensing electric field.

Assuming that the magnitude of the imaginary part of the dielectric permittivity of the studied material is attributable to the phase difference between the mixed forced-free oscillations of the electronic subsystem of the crystalline material and the current flowing through the sample, it can be argued that the maximum phase shift should be observed under quasi-resonance conditions.

Thus, at frequencies significantly lower than the resonant frequency, the slowly changing external sinusoidal electric field is completely displaced into the mica substrate by an array of free electrons in the crystal VO_2, since the concentration of free electrons in both the semiconductor and metallic phases is many orders of magnitude higher than the concentration of free electrons in mica. Obviously, in the process of such displacement, the above-mentioned phase shift is minimal, since the Maxwell relaxation time is so short that displacement occurs almost instantly with virtually no phase shift.

At frequencies significantly exceeding the inverse Maxwell relaxation time, the process of displacement of the external probing field into the mica substrate manages to develop only in its infancy, since the initial phase of displacement is confronted with the fact that the external sinusoidal field has already changed its sign. Obviously, at the initial stage, the phase shift mentioned above is also small.

It follows from the above that the maximum phase shift should be expected at a certain „resonant“ frequency due to the coincidence of the oscillation frequency of the external field and the frequency of Maxwell relaxation of the crystal VO_2. The maximum occurs due to the fact that the process of interaction of the array of free electrons of the crystal with the external probing field has time to form effectively, and the field has not yet been displaced into the substrate. Under the conditions of such resonance, the loss of electrical energy, called dielectric losses, is maximum. The nature of the mechanism of energy losses in such processes is different for doped and undoped crystals.

Thus, the proposed model relates the formation of DS features, in particular, the maxima of the function $\varepsilon''(f)$, to the presence of free electrons in the crystalline grains of the VO_2 film. When an external probing electric field is applied to the film, the electrons shift (drift) and displace the field applied to the film into the dielectric substrate. The „resonance“ of such a process occurs at a frequency of $f = 2\pi\omega = 2\pi/\tau_{\text{m}}$, where $\tau_{\text{m}} = \varepsilon\varepsilon_0/\sigma$ is the Maxwellian relaxation time, σ is the specific conductivity of the film grain. The grains of the film VO_2 are in the monoclinic phase with a low concentration of free electrons and, consequently, a low grain conductivity far from the PT temperature ($T_{\text{c}} = 67\,^\circ\text{C}$) at $T = 50\,^\circ\text{C}$. The Maxwellian time is relatively long, and the maximum of the function $\varepsilon''(f)$ and the step $\varepsilon'(f)$ are located in the region of relatively low frequencies $f = 10^{4.5}\,\text{Hz}$ (Figure 1). As the temperature increases, the concentration of free electrons in the monoclinic phase and the specific conductivity σ

of crystal grains increase, the time τ_{m} decreases, and the resonant features of the DS shift towards high frequencies, which is observed in the experiment.

Doping of films with various elements (n-type or p-type impurities) changes the electrical characteristics of the film grains, affecting the value of σ and, thereby, the DS parameters.

The temperature range considered in the article is the area of the semiconductor-metal thermal PT in VO_2. As already noted in the introduction, PT has a complex character in vanadium dioxide characterized by the fact that the Peierls structural PT is preceded by the Mott electron transition, which occurs over a wide temperature range and stimulates the Peierls structural PT. The Motta PT is an electronic PT caused by a narrowing of the band gap with the increase of the temperature due to the so-called strong electron-electron correlations and, as initially assumed, does not have thermal hysteresis. Peierls PT is a rearrangement of the crystal lattice structure, accompanied by an abrupt change of the symmetry of the crystal structure of each grain of the film with temperature variation in the PT region. As the temperature increases for grains of different sizes, the transition of the crystal VO_2 from the monoclinic phase to the tetragonal phase occurs at different temperatures, by varying the amounts exceeding the temperature of $T_c = 67\,^\circ\mathrm{C}$ experimentally observed for the PT of an infinite single crystal of VO_2. As the temperature decreases, the reverse transition also occurs at different temperatures, which are lowered differently for grains of different average sizes. This means that the semiconductor-metal PT is characterized by temperature hysteresis. A comparative analysis of the shape and thermal position of the temperature hysteresis loops for doped and undoped films of VO_2 allows drawing important conclusions about the mechanism of the effect of dopants on the PT process.

Thus, the experiment shows that weak doping (less than 3 %) of films of VO_2 with silver broadens the features of DS over the occupied frequency range and increases the temperature of PT by $10\,^\circ\mathrm{C}$ (shifts the temperature hysteresis loop towards high temperatures by $10\,^\circ\mathrm{C}$). Strong silver doping (of the order of 6 %) leads to the appearance at low frequencies ($10^2-10^{3.5}$ Hz) of an additional maximum $\varepsilon''(f)$ and an additional step $\varepsilon'(f)$, the shape and frequency position of which does not depend on temperature. The loop of temperature hysteresis of the „old" maximum additionally shifts towards high temperatures only by $5\,^\circ\mathrm{C}$.

Thus, doping of the VO_2 film with silver ions increases the temperature of the PT material from the semiconductor to the tetragonal phase, which, according to the proposed model of the processes, is the result of the formation of Ag-Ag-dimers, which are more durable than V-V-dimers of undoped crystal of VO_2. Namely, a double bond occurs between silver ions in neighboring oxygen octahedra with σ and π components. Let's consider the mechanism of bond formation in more detail.

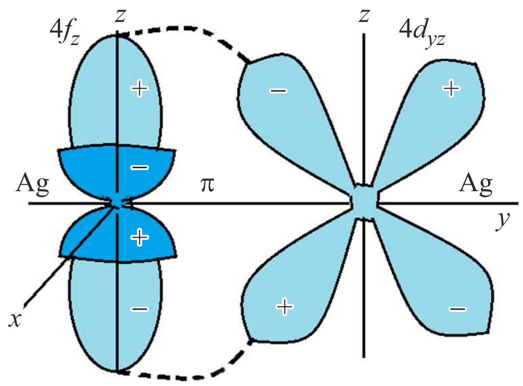

Figure 7. Scheme of formation of additional π bonds in Ag-Ag-dimers.

A nanocrystalline film of VO_2 doped with silver ions is synthesized at a temperature of 700−900 K. This circumstance creates the possibility of migration of silver ions in the film over the surface of the substrate, which minimizes the Gibbs free energy during the formation of the crystal lattice. Energy minimization promotes the formation of impurity pairs in the doped material that lower energy, namely, Ag−Ag-dimers.

Ag^{4+} ions replace V^{4+} ions in the center of the base of the oxygen octahedron during doping. Ag atom has the following electronic configuration: $1s^22s^22p^63s^23p^64s^23d^{10}4p^65s^14d^{10}$ [14]. Ag^{4+} ions delegates the following 6 atomic orbitals to create σ bonds with corner O^{2-} ions: $4d^2_{z2}4d^2_{xy}4f^0_{x(x2-y2)}4f^0_{z(x2-y2)}4f^0_{xz2}4^0f_{yz2}$. They contain 4 electrons to form 6 hybrid orbitals. At the same time, each hybrid orbital of the Ag^{4+} ion located in the center of the base of the oxygen octahedron, as for the V^{4+} ion, accounts for an average of 2/3 of the electron density, which, together with 4/3 of the electron density of the corner ion O_2, creates full-fledged σ-bonds that ensure the stability of the crystal lattice.

The Ag atom is a strongly correlated element, the energy position of the levels of which strongly depends on their population of electrons. For this reason, the $4d$-shell of a silver atom, having 9 electrons, can accept one electron for its final filling, and the $5s$-shell retains only one electron.

$5s^1$ — orbital containing a single electron that does not participate in hybridization can form a standard σ-bond in the semiconductor phase of VO_2 with a similar orbital of the Ag^{4+} ion located in the center of a neighboring oxygen octahedron. It follows from the above that the proposed model assumes, as indicated above, the formation of $Ag^{4+}-Ag^{4+}$-dimers. However, this bond is less strong than $3d_{x2-y2} - 3d_{x2-y2}$ — σ-bond in V-V-dimers of an undoped crystal, which is attributable to the increased electron shielding of the inner shells of the Ag^{4+} ions. Therefore, it cannot ensure the experimentally observed increase of the PT temperature in case of doping of VO_2 films with silver ions. The proposed model explains this phenomenon by indicating the possibility of increase of the strength of Ag-Ag-dimers due to the formation of an additional coordination π-bond between silver ions of neighboring octahedra.

That is, the problem of insufficient strength of the $5s$-$5s$-σ-bond for increasing T_c is resolved as follows. An additional π-bond, which increases the strength of Ag-Ag-dimers compared to V-V-dimers, is ensured by the fact that one of the orbitals of the $4d$-shell of silver ion creates a donor-acceptor π-bond with one of the free orbitals of the $4f$-shell of the adjacent Ag^{4+} ion: for example, π-bond of $4d^2_{yz} - 4f^0_{z3}$ type (Figure 7).

Let's pay attention to the fact that these orbitals belong to the same 4-th layer. This observation is significant because molecular orbital theory prohibits the formation of σ-bonds between different shells of the upper electron layers due to their instability, which arises from the poor overlap of differently sized orbital lobes.

6. Conclusion

The mechanism of the effect of film doping with silver atoms on their electrical properties and on the PT processes occurring in nanocrystallites is as follows.

With weak doping (about 3,%), a small number of strong Ag-Ag-dimers replacing V-V-dimers reduces the concentration of free equilibrium electrons and thereby reduces the specific conductivity of grains. An increase of the total bond strength inside the dimers that stabilize these dimers, according to the conclusions of the theory of molecular orbitals, increases the energy gap between d_{bott} and d_{top} electron bands. That is, d_{bott} decreases in energy, and d_{top} increases in energy. At the same time, the energy gap between the d_{bott} and π^*-bands (i.e., the band gap of the crystal) increases not only because the lower Hubbard zone d_{bott} decreases in energy, as indicated. But also because the $4d_{\text{yz}}$ orbital is occupied and is now used to strengthen Ag-Ag-dimers. This implies that for the formation of the π^*-band (unlike V–O — π-bonds), only the $4d_{\text{xz}}$-orbital remains, which forms a π-bond with the $2p_z$-orbital of the corner oxygen ion and creates the energy gap between the π and π^* bands. This process slightly moves both these bands up in energy closer to the vacuum level, forcing the linking π-band to approach the d_{bott}-band from below, and the π^*-band to move away from it. The movement of the d_{bott}-band and π^*-band in opposite directions increases the band gap of the material, impoverishing the conduction band with electrons. As a result, the DS features become wider in frequency, the band gap becomes even wider due to correlation effects, the initiation of structural PT occurs at a higher temperature, and the temperature hysteresis loop shifts towards high temperatures by 10 °C (according to the experiment).

Two types of grains are formed with significantly different values of the specific conductivity of the grains in case of a heavy doping with silver (about 6 %): most of the grains are heavily doped, the second part, as in the previous case, is weakly doped. A large number of strong Ag-Ag-dimers are formed in heavily doped grains, which retain electrons and thereby further reduce the concentration of free electrons in the conduction band. Therefore, the specific conductivity of such grains is small, their corresponding frequency features are located at low frequencies, these dimers do not destabilize with the increase of the temperature, structural PT does not occur at $T_c = 67\,^\circ\text{C}$, and the specific conductivity practically does not change with temperature. As for the second part of the grains, the change of their properties and the temperature behavior of the DS features remains similar to the case of weakly doped films described above, but the temperature hysteresis loop σ still additionally shifts towards high temperatures by another 5 °C and acquires an asymmetric shape. The asymmetry is associated, as has already been observed with doping with other impurities, with a systematic shift of T_c in doped grains towards high temperatures, and this consistency is typical for grains with wide hysteresis loops. The reason lies in the p-type properties of impurity ions, which, as indicated above, deplete the conduction band due to the corresponding energy shifts of the bands, which increases T_c and is most pronounced in severely defective grains, such as grains with small sizes. That is, in such grains there is a correlation between a systematic increase of the temperature T_c of the phase equilibrium and the width of the elementary hysteresis loops, which increases with a decrease of the grain size. This creates an asymmetry in the overall hysteresis loop, which is observed experimentally.

Conflict of interest

The authors declare that they have no conflict of interest.

References

[1] W. Bruckner, H. Opperman, W. Reichelt, E.I. Terukov, F.A. Tschudnovskii. Vanadiumdioxide. Berlin, Akamemie-Verlag, (1983).

[2] N.F. Mott. Perekhody metall-izolyator. M., Nauka (1979). (in Russian).

[3] A.A. Bugaev, B.P. Zakharchenya, F.A. Chudnovsky. Fazovyj perekhod metall–poluprovodnik i ego primenenie. L., Nauka (1979). (in Russian).

[4] S. Shin, S. Suga, M. Taniguchi, M. Fujisawa, H. Kanzaki, A. Fujimori, H. Daimon, Y. Ueda, K. Kosuge, S. Kachi. Phys. Rev. B, **41**, 4993 (1990).

[5] E.B. Shadrin, A.V. Ilyinsky. FTT **42**, *6*, 1092 (2000). (in Russian).

[6] A.V. Ilinskiy, R.A. Kastro, M.E. Pashkevich, E.B. Shadrin. FTP **54**, *2*, 153 (2020). (in Russian).

[7] A.V. Ilyinsky, R.A. Castro, V.A. Klimov, A.A. Kononov, E.B. Shadrin, Optika i spektroskopiya, bf 130, it 10, 1491 (2022). (in Russian).

[8] E.B. Shadrin, A.V. Ilyinsky, R.A. Castro, V.M. Kapralova, A.A. Kononov, M.E. Pashkevich, NTV SPbGU. Fiziko-matematicheskie nauki, **15**, *4*, 7, (2022). (in Russian).

[9] A.R.A. Castro, A.V. Ilinskiy, V.A. Klimov, M.E. Pashkevish, E.B. Shadrin, Phys. Complex Systems, **3**, *1*, 43 (2022).

[10] R.A. Castro, A.V. Ilyinsky, M.E. Pashkevich, A.A. Kononov, V.A. Klimov, E.B. Shadrin, Dielektricheskaya spektroskopiya tonkikh plenok oksidov vanadiya, legirovannykh primes'yu metallov. Monografiya. p. 167. (2023) Herzen Russian State Pedagogical University, Pavlov Institute of Physiology, Russian Academy of Sciences, Saint Petersburg ISBN: 978-5-9031-8781-2. (in Russian).

[11] A.M. Prokhorov. Dielekticheskie izmereniya. M. (1988). V. 1. P. 700. (in Russian).

[12] S. Havriliak, S. Negami J. Polym. Sci. C. **14**. 99 (1966).

[13] A.V. Ilyinsky, E.B. Shadrin, FTT, **66**, *5*, 708 (2024).

[14] B.F. Ormont. Vvedenie v fizicheskuyu khimiyu i kristallokhimiyu poluprovodnikov. Izd. „Vysshaya shkola", M. p. 658. (1973). (in Russian).

Translated by A.Akhtyamov